A practical approach to quantify the ADF detector in STEM

D. S. He and Z. Y. Li*

Nanoscale Physics Research Laboratory, School of Physics and Astronomy, University of Birmingham, Birmingham B15 2TT, UK

*Email: z.li@bham.ac.uk

Abstract. We present a practical approach to quantify the annular dark field (ADF) detector in scanning transmission electron microscope (STEM). The non-uniform response of the detector as a function of the beam current is investigated. The brightness and contrast of the preamplifier have been taken into account to find the black level of the detector. The efficiency map is obtained.

1. Introduction

Quantitative analysis of annular dark field (ADF) image in scanning transmission electron microscopy (STEM) is useful in the three dimensional characterisation of the nano-object [1-3]. Here, the performance of the ADF detector is crucial and the quantification procedure is necessary for the quantitative analysis of ADF-STEM. So far, several procedures have been reported [3-5]. These procedures made use of additional calibrated instruments, either the dynamical signal analyzer [4] or Faraday cup [5], but none had taken into account of the non-uniformity of the detector in quantification [3-5].

In this work, we present a practical approach to characterise the performance of the ADF detector. By varying the beam dose, we identify a linear response region of the detector and find the black level of the detector. We then obtain the efficiency map of the detector.

This work is conducted on the JEOL2100F, with CEOS probe corrector, located in the University of Birmingham. The JEOL ADF detector is a P47 phosphor scintillator disk with a hole in the center, whose inner and outer diameters are 3 and 8 mm respectively. The brightness and contrast of the detector can be controlled by the software. The charge coupled device (CCD) camera installed is Gatan 2k × 2k UltraScan1000 with the conversion factor of 0.266 electron/count provided by the manufacturer.

2. The electron beam dose measurement

In the present study, the CCD camera is used to measure the e-beam dose. The response of the camera is shown in Figure 1: (a) is an image taken with 7s exposure time when the specimen was removed from the field of view and the beam was spread evenly across the CCD sensor. At this exposure time, the CCD is at about half of its full dynamic range. (b) is the intensity line profile showing that the CCD has a low background level. (c) is the count rate integrated over the entire CCD, after background subtraction, as a function of the exposure time. The dashed line is a linear fit with the

function of $y = ax$ for exposure time less than ~13s. The linear response of the CCD camera enables us to work out the beam current by dividing the total number of electrons reaching the CCD (counts × 0.266) by exposure time. Table 1 shows typical values of the beam current obtained in this way, with emission current of 138 μA, for different condenser aperture sizes and spot sizes. Here aperture 4 and 3 are the smallest and the second smallest aperture of the microscope. The CCD camera saturates at ~65000 counts per pixel.

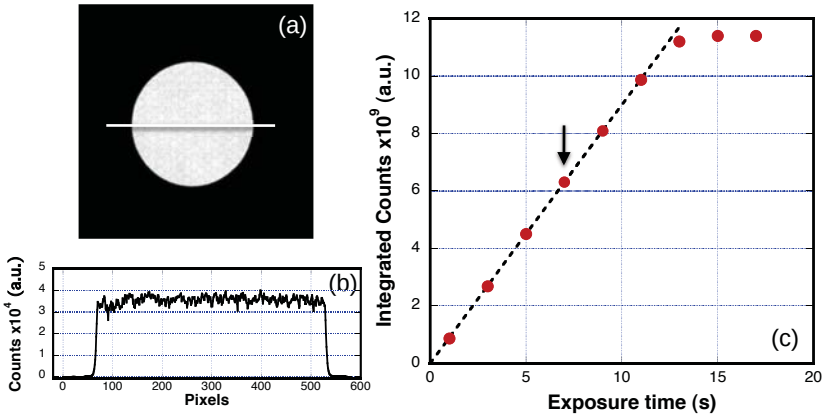

Figure 1 The linear response of CCD camera. (a) An image of the CCD taken when the specimen was removed from the field of view. (b) The line profile intensity indicated in (a). (c) The counts integrated over the entire CCD as a function of exposure time.

Table 1 The beam current for the typical microscope setting

Aperture	4					3				
Spot size	10C	9C	8C	7C	6C	10C	9C	8C	7C	6C
Beam current (pA)	5.6	8.4	16.5	24.5	50.1	11.5	17.9	35.1	52.9	108.3

3. The performance of the ADF detector as a function of the beam dose

Fig. 2 (a) shows the response of the JEOL ADF detector by focusing the electron beam directly on it. It is clear that the response of the detector is non-uniform. For the same beam current, the upper left region near the inner boundary has the highest output count and the lower right region near the outer boundary has the lowest output count. The output counts at three locations, indicated respectively by the dot, square and diamond in Fig. 2 (a), were investigated as a function of beam current. Here, the beam current was varied by changing aperture size and spot size as calibrated in Section 2. The results are shown in Fig. 2 (b) with the same symbols. In general, for each location, there are three operating regions: a region that has zero counts when the electrons reach the detector (cut-off region); a region where the output count is linear to the incident beam current (linear region, fitted with lines) and a region where the count is saturated (saturation region). Operating in both the cut-off and the saturated regions leads to distortion of the linearity of the data, which should be avoided.

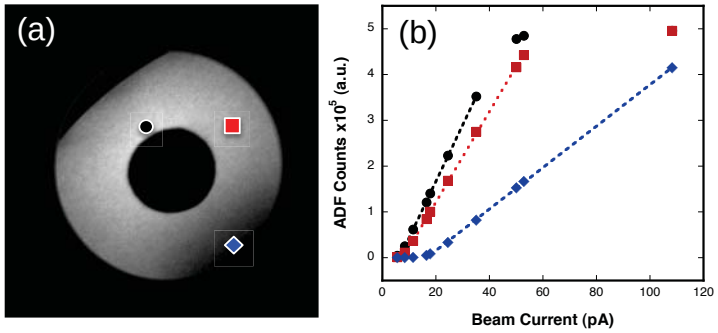

Figure 2 (a) An example of the scanning of the ADF detector. (b) The highest, intermediate and the lowest response of the detector as a function of beam current.

4. The influence of the brightness and contrast setup

The setting of the brightness and contrast of the preamplifier can change the output count of the ADF detector. Two important parameters are considered: the X-intercept and slope (as indicated in Figure 3 (a)). It is found that the X-intercept represents the electron dose that must be exceeded to generate counts. The X-intercepts and slopes differ from one position to another on the detector. Figure 3 (b, c) and (e, f) show the slope and X-intercept as a function of the brightness and contrast respectively, with dashed curves showing fits. The fitting functions used are $y = a$ in (b) and (d), $y = ax+b$ in (c) and $y = be^{ax}$ in (e) and (f), where a and b are constants and x and y are variables. Figure 3 (b) shows that the brightness has little influence on the slope and has a linear relationship with the X-intercepts shown in Figure 3 (c). As indicated in the dashed circle in Fig. 3 (c), the intercepts of three locations all reach zero at brightness of about 2900, showing that every electron contributes proportionally to the output counts. With this setup, the count read out can be linked to the number of electrons arriving at the particular location of the ADF detector.

The relationship between contrast and the slope, as well as contrast and the X-intercept, is not linear. As shown in Figure 3 (e) and (f), the slopes increase exponentially as a function of contrast while the X-intercepts decrease exponentially against the contrast. This is because that the X-intercept is equal to the offset level of the detector divided by the slope as indicated in Figure 3 (a). However, the relative slopes (the relative conversion factors) stay unchanged as the contrast setup is varied (Figure 3 (d)). If the offset was zero, i.e. at brightness of 2900, the relative slopes would be the same because there is no cut-off region, thus the count-current curves would pass through the origin. As a result, the relative conversion factor can be mapped directly by scanning the entire detector area. Alternatively, the slope must be extracted from fitting to the linear operating region for each location of the detector.

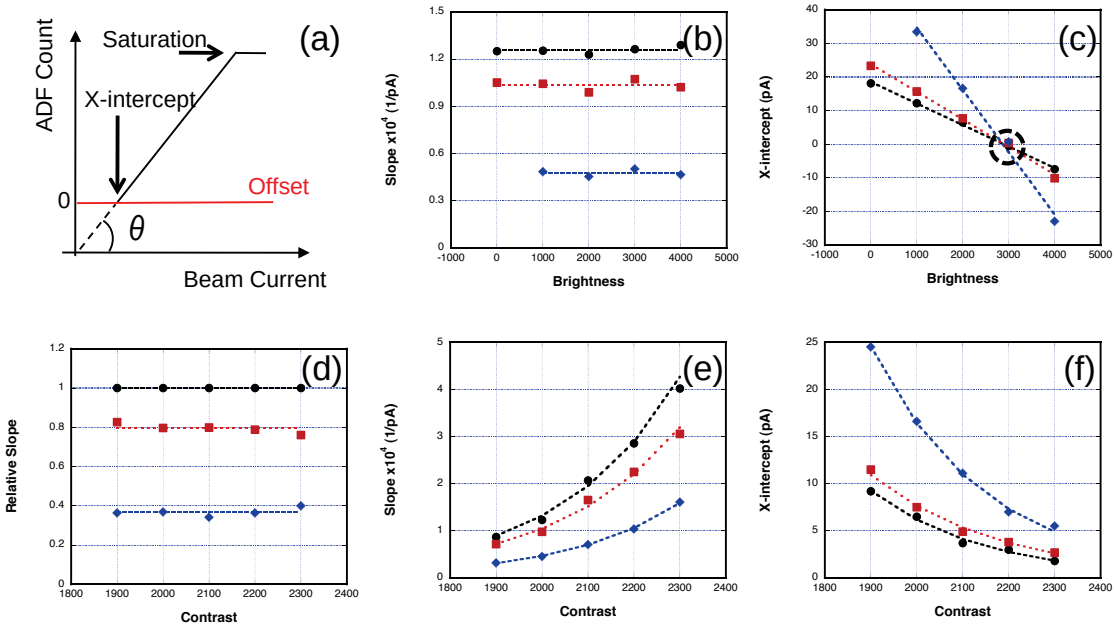

Figure 3 (a) A schematic of the ADF response as a function of beam current. (b) The slope as a function of brightness at contrast = 2000. (c) The X-intercept as a function of brightness at contrast = 2000. (d) The relative slope as a function of the contrast at brightness = 2000. (e) The slope as a function of contrast at brightness = 2000 (f) The X-intercept as a function of contrast at brightness = 2000. In (b-f), the dots, squares and diamonds are from the highest, intermediate and lowest efficiency locations indicated in Figure 2 (a).

5. The efficiency map

The conversion factor (the number of electrons to ADF counts) has been mapped point by point as follows: (1) the response was mapped at different beam currents and aligned using a correlation coefficient; (2) at each position, after being averaged over 10×10 pixels windows, the linear range was fitted with a linear function; (3) the slope of the fitting parameters was obtained and normalised to the largest slope. The obtained detector map would be slightly distorted if the beam was not perfectly aligned. In Figure 4 (a), the geometrical distortion of the mapping has been corrected, assuming the detector has a perfectly round shape. The circularly averaged response of the ADF detector is shown in Fig. 4 (b) where it can be seen that for most parts of the detector the efficiency is between 0.6-0.8. It is worth mentioning that the map in Fig. 4 (a) shares similar characteristic detector features as the map shown in Fig. 2 (a), which is obtained by scanning the detector using a fixed beam current. The non-uniformity of ADF detectors is common when compared to other commercially available microscopes, though with varying degree [3-5]. This is likely a result of current design geometry.

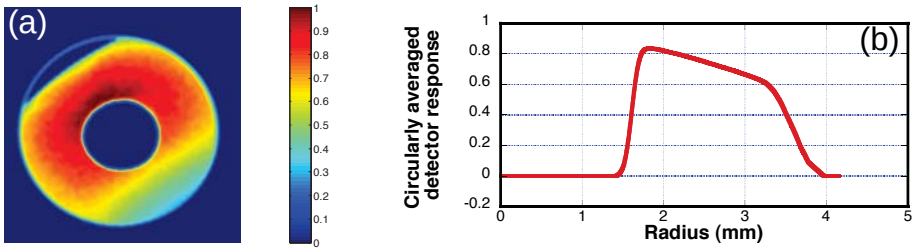

Figure 4 (a) The efficiency map of the detector. (b) The circularly averaged efficiency.

6. Conclusion

We have described a practical approach to quantify the ADF detector. Through a detailed analysis of detector response rate, we obtain the efficiency map which has taken into consideration the non-uniformity of the detector. This method can be applied to most commercially available microscopes which are not fitted with a Faraday cup. By analysing the response of the detector as a function of beam current, we find that though the detector response is not uniform, it is linear within certain beam current regions. By varying the brightness and contrast of the preamplifier, we find that different regions of the detector share the same black level (at brightness=2900). The brightness and contrast do not change the relative efficiency of the detector. Such an efficiency map would be useful when the absolute electron scattering cross-section is needed for quantitative comparisons between experimentally recorded and simulated images [7].

7. Acknowledgements

We acknowledge the financial support from the EPSRC. The STEM instrument employed in this research was obtained through the Birmingham Science City project. DSH acknowledge the studentship from the University of Birmingham and the China Scholarship Council.

References

[1] Li Z Y et al. 2008 Nature **451** 46.
[2] Young N P et al. 2008 Physical Review Letters **101** 246103.
[3] Katz-Boon H et al. 2013 Ultramicroscopy **124** 61.
[4] LeBeau J M and Stemmer S 2008 Ultramicroscopy **108** 1653.
[5] E H et al. 2010 Jounal of Physics: Conference Series **241** 012067.
[6] JEOL Instruction Manual 2007 (EM-24560)
[7] Findlay S D and LeBeau J M 2013 Ultramicroscopy **124** 52.